Secondary inorganic aerosols in Europe: sources and the significant influence of biogenic VOC emissions especially on ammonium nitrate

Sebnem Aksoyoglu, Giancarlo Ciarelli, Imad El-Haddad, Urs Baltensperger and André S. H. Prévòt

Laboratory of Atmospheric Chemistry, Paul Scherrer Institute, 5232 Villigen PSI, Switzerland

5   *Correspondence to*: Sebnem Aksoyoglu (sebnem.aksoyoglu@psi.ch)

Abstract Contributions of various anthropogenic sources to the secondary inorganic aerosol (SIA) in Europe as well as the role of biogenic emissions on SIA formation were investigated using the three-dimensional regional model CAMx (Comprehensive air quality model with extensions). Simulations were carried out for two periods of EMEP field campaigns (February-March 2009 and June 2006), which are representative of cold and warm seasons, respectively. Biogenic volatile organic compounds (BVOCs) are known mainly as precursors of ozone and secondary organic aerosol (SOA), but their role on inorganic aerosol formation has not attracted much attention so far. In this study, we showed the importance of the chemical reactions of BVOCs and how they affect the oxidant concentrations leading to significant changes in inorganic nitrate and sulfate. A sensitivity test with doubled BVOC emissions in Europe during the warm season showed a large increase in secondary organic aerosol (SOA) concentrations (by about a factor of two) while particulate inorganic nitrate concentrations decreased by up to 35%. Sulfate concentrations decreased as well, the change, however, was smaller. The changes in inorganic nitrate and sulfate concentrations occurred at different locations in Europe indicating the importance of precursor gases and biogenic emission types for the negative correlation between BVOCs and SIA. Further analysis of the data suggested that reactions of the additional terpenes with nitrate radicals at night were responsible for the decline in inorganic nitrate formation, whereas oxidation of BVOCs with OH radicals led to a decrease in sulfate. Source apportionment results suggest that the main anthropogenic source of precursors leading to formation of particulate inorganic nitrate is road transport (SNAP7), whereas combustion in energy and transformation industries (SNAP1) was the most important contributor to sulfate particulate mass. Emissions from international shipping were also found to be very important for both nitrate and sulfate formation in Europe. In addition, we examined also contributions from the geographical source regions to SIA concentrations in the most densely populated region of Switzerland, the Swiss Plateau. The results suggest that sources of particulate sulfate were mostly of foreign origin (the domestic contributions were 11% and 3% in winter and summer, respectively). On the other hand, about 20% of the particulate nitrate was from domestic sources while contributions from the neighboring countries Germany and France were significant as well. Particulate ammonium was estimated to originate mainly from local agricultural activities.

1 Introduction

Particulate matter (PM) is known to have adverse effects on human health and climate, and is still a problematic pollutant in Europe in spite of considerable improvements in the last decades (Barmpadimos et al., 2012; EEA, 2014). The sources and evolution of PM in the atmosphere are among the most extensively investigated topics in current atmospheric research (Fuzzi et al., 2015; Denier van der Gon et al., 2015). PM is either directly emitted or formed in the atmosphere as secondary inorganic (SIA) and organic aerosols (SOA). The main precursor gases for SIA are SO_2, NO_x and NH_3, which react in the atmosphere to form ammonium sulfate and nitrate compounds. Observations from the EMEP network show that SIA concentrations in Europe increase from north to south, with an average contribution of 34% to PM_{10} (particles with an aerodynamic diameter $d < 10$ µm) mass (Aas et al., 2012). Earlier studies suggest that SIA constitutes more than half of $PM_{2.5}$ ($d < 2.5$ µm) concentrations in Europe, especially in winter (Schaap et al., 2004; Aksoyoglu et al., 2011; 2012; Squizzato et al., 2013).

A combination of meteorological conditions and various emission sources led to highly elevated PM concentrations in Europe during early spring episodes in the past, mainly due to high ammonium nitrate concentrations (Sciare et al., 2010; Revuelta et al., 2012). Knowing the location and strength of sources contributing to $PM_{2.5}$ is essential for developing effective control strategies. Although the inorganic aerosol system of sulfate, nitrate and ammonium is well understood, chemical transport models (CTMs) usually overestimate nitrate concentrations. This is believed to be due to uncertainties in NH_3 emissions (Aan de Brugh et al., 2011; Wang et al., 2013) while the effect of uncertainties in NO_x emissions and transformation cannot be ruled out (Vaughan et al., 2016).

On the other hand, biogenic emissions have even a larger uncertainty than the anthropogenic ones (Sindelarova et al., 2014; Emmerson et al., 2016). However, their role on SIA formation has not attracted much attention so far. Biogenic species such as isoprene, mono- and sesquiterpenes emitted from vegetation are known mainly as precursors of secondary pollutants like ozone and SOA (Kanakidou et al., 2005; Sartelet et al., 2012). The nitrate radical is an effective nocturnal oxidizer of VOCs and it is especially reactive towards biogenic volatile organic compounds (BVOCs). Laboratory experiments showed a rapid production of SOA with high yields when some monoterpenes were

oxidized by nitrate radicals (Fry et al., 2011; Boyd et al., 2015). Although there has been extensive research on formation of SOA from oxidation of BVOC (Carlton et al., 2009; Hallquist et al., 2009; Ayres et al., 2015; Xu et al., 2015; Fuzzi et al., 2015), to our knowledge, effects of BVOC on SIA, especially nitrate, have been scarcely investigated (Karambelas, 2013). The goals of this study are (1) to

5 identify various types of emission sources of SIA as well as their locations during cold and warm seasons and (2) to investigate the correlation between BVOCs and formation of secondary inorganic aerosols in Europe.

2 Modeling Methods

2.1 Air quality model CAMx

10 In this study, we used the regional air quality model CAMx-v5.40 with its PSAT (Particulate Source Apportionment Technology) tool (ENVIRON, 2011). The model domain covered Europe using latitude-longitude geographical coordinates with a horizontal resolution of 0.25° x 0.25°. We used 33 terrain-following σ-levels up to about 350 hPa. The Carbon Bond (CB05) gas phase mechanism (Yarwood et al., 2005) was used and partitioning of inorganic aerosols (sulfate, nitrate, ammonium, sodium and

15 chloride) was performed using the ISORROPIA thermodynamic model (Nenes et al., 1998). Aqueous sulfate and nitrate formation in cloud water was simulated using the RADM aqueous chemistry algorithm (Chang et al., 1987). Partitioning of condensable organic gases to secondary organic aerosols (SOA) was calculated using the semi-volatile equilibrium scheme called SOAP (Strader et al., 1999). SOA precursor species and reactions are given elsewhere (Aksoyoglu et al., 2011). Removal processes

20 including dry and wet deposition were simulated using the Zhang resistance model (Zhang et al., 2003) and a scavenging model approach for both gases and aerosols (ENVIRON, 2011).

Input parameters for CAMx were provided by INERIS within the EURODELTA III project (Bessagnet et al., 2014). Hourly three-dimensional meteorological fields for wind speed and direction, pressure, temperature, specific humidity, cloud cover and rain were calculated from ECMWF IFS (Integrated

25 Forecast System) data at 0.2° resolution within the EURODELTA III exercise. MACC (Monitoring Atmospheric Composition and Climate) reanalysis data were used to generate initial and boundary

condition fields (Benedetti et al., 2009; Inness et al., 2013). Photolysis rates were calculated using the Tropospheric Ultraviolet and Visible (TUV) Radiation Model (https://www2.acom.ucar.edu/modeling/tropospheric-ultraviolet-and-visible-tuv-radiation-model). The ozone column densities to determine the spatial and temporal variation of the photolysis rates were

5   extracted from TOMS data (https://ozoneaq.gsfc.nasa.gov/data/omi/). Anthropogenic emissions were prepared by merging different emission databases such as TNO-MACC (Kuenen et al., 2011), EMEP (Vestreng et al., 2007) and GAINS (http://gains.iiasa.ac.at/gains) as described in Bessagnet et al. (2014). We calculated the gridded biogenic VOC emissions using the Model of Emissions of Gases and Aerosols from Nature (MEGAN v2.1) (Guenther et al., 2012) driven by the meteorological variables.

10   We ran CAMx with PSAT for the two EMEP intensive measurement campaign periods: 25 February-26 March 2009 (cold season) and 1-30 June 2006 (warm season) with a 14-day spin-up before each period. The model results for aerosols in this study refer to $PM_{2.5}$ fraction. In order to investigate the role of biogenic emissions on the SIA formation, we doubled the BVOC emissions in June 2006 in the model domain and repeated the simulations. We analyzed the model results by means of the Chemical Process

15   Analysis (CPA) tool of CAMx, which provides detailed reaction rate information for selected species from various chemical reactions.

2.2 Particulate Source Apportionment Technology (PSAT)

Source apportionment techniques are used to identify the sources of atmospheric pollutants (Viana et al., 2008). It is relatively simple to apportion primary PM among its sources using any pollution model

20   because their source-receptor relationships are linear. On the other hand, Eulerian models are better suited to model secondary PM because they account for chemical interactions among sources. The CAMx tool PSAT was used to assess the contribution of different geographic regions and source categories to modeled concentrations of SIA. PSAT uses reactive tracers to apportion primary and secondary PM as well as the gaseous precursors among different source categories and regions. A single

25   tracer can track primary PM species, whereas secondary PM species require several tracers because of the more complex relationship between gaseous precursors and the resulting particles. PSAT assumes that PM should be apportioned to the primary precursor for each type of particle. Thus particulate

sulfate (PSO$_4$) is apportioned to SO$_x$ emissions, particulate nitrate (PNO$_3$) is apportioned to NO$_x$ emissions, and particulate ammonium (PNH$_4$) is apportioned to NH$_3$ emissions (ENVIRON, 2011). We defined source categories (Table 1) based on the SNAP codes given by Kuenen et al. (2011). We also modeled the contribution from the boundaries of the domain as a non-European source.

5 In addition to source categories, we also investigated in a case study the contribution from various source regions to SIA concentrations in the Swiss Plateau, which is the most densely populated part of Switzerland, comprising the area between the Jura Mountains and the Swiss Alps (Fig. S1). The selected source regions were identified as Switzerland (domestic), France, Germany, Italy and Austria (surrounding countries), Poland and Benelux countries (polluted regions), Sea (marine areas), Rest (rest

10 of the domain), and BC (boundary conditions) (see Fig. S2).

Measurements with the high resolution AMS (Aerosol Mass Spectrometer) are available at 11 European sites for the February-March 2009 period (Crippa et al., 2014). A detailed evaluation of CAMx model performance for the two periods simulated in this study can be found elsewhere (Ciarelli et al., 2016). Since AMS data are only available at Payerne for the summer June 2006 period, we evaluated

15 meteorological parameters and SIA concentrations at that site in both cold and warm seasons.

3 Results and discussion

3.1 Model evaluation

The temporal variations of both meteorological parameters and chemical components were captured quite well by the model (Figs. S3-S4). There is a clear correlation between the SIA concentrations and

20 wind speed. In the cold season, agreement between modeled and measured wind speed is very good (Fig. S3); concentrations are higher when the wind speed is low (25 February-5 March, 18-19 March, and 22-23 March). The modeled SIA concentrations are very close to the measured ones, except for a few days (3 and 23 March). As part of the EURODELTA III project, Bessagnet et al. (2014) analyzed measured and modeled meteorological variables such as PBL height and wind speed at several sites in

25 Paris. The study suggested that observations were well reproduced by ECMWF IFS in general except for a few days when the PBL height was overestimated (Bessagnet et al., 2014). The modeled SIA

concentrations during the warm season were also very close to measurements except for an overestimation during the first week when temperatures were relatively lower (Fig. S4, right panel). Underestimated wind speed and PBL height might be some of the reasons of this discrepancy. A slight underestimation of temperature might also have caused more partitioning on the particle phase.

5 3.2 Particulate Nitrate (PNO$_3$)

The modeled PNO$_3$ concentrations were higher in the cold season with a monthly average of up to 14 µg m^{-3} over northern Italy (Fig. 1, top left). In the warm season, highest concentrations (7-8 µg m^{-3}) were predicted mainly around the English Channel and Benelux area (Fig. 1, top right). The largest contribution to nitrate was from road transport, followed by ships and combustion in energy and

10 transformation industries while the contribution from the boundaries was very small (Fig. 1). The relative contribution from road traffic was higher in Eastern Europe (Fig. S5). The contribution of SNAP 1 sources to PNO$_3$ was higher in East European countries during the cold season (Fig. 1). The relative contribution from offshore petroleum activities in the North Sea to PNO$_3$ was quite high as seen in Fig. S5. Emissions from the petroleum sector are generally exhaust gases from combustion of natural

15 gas in turbines, flaring of natural gas and combustion of diesel. Ship emissions (SNAP8) in the warm season led to PNO$_3$ formation mainly along the English Channel, whereas their contribution in the cold season was predicted throughout the whole of Central Europe, most likely because of higher NH$_3$ emissions in this area in the early spring. This agrees with the results of previous simulations (Aksoyoglu et al., 2016). On the other hand, the relative contribution from ship emissions to PNO$_3$ was

20 clearly higher over the Mediterranean in both seasons (Fig. S5).

3.3 Particulate Sulfate (PSO$_4$)

The modeled particulate sulfate concentrations were relatively low over central Europe during the cold season (Fig. 2). A significant contribution, however, was detected from the eastern boundaries of the model domain (for relative contributions see Fig. S6). The effect of boundary inflows on sulfate levels

25 in the warm season was much lower. Emissions from the combustion in energy and transformation industries are the main sources for particulate sulfate in Eastern Europe, while shipping contributes

mainly in the Mediterranean and along other shipping routes around Europe (Fig. 2). Significant contributions from SNAP1 sources in June were predicted over the Balkan countries as well as in northwest Spain (Fig. S6) where large facilities are grouped (Guevara et al., 2014). The contribution from ships to PSO_4 was predicted to be larger during the warm season. Although ship emissions are

5   only slightly higher in summer, their larger contribution to sulfate is mainly due to higher oxidation potential in the warm season (Aksoyoglu et al., 2016).

3.4 Particulate Ammonium (PNH_4)

The modeled PNH_4 concentrations were relatively higher during the period of February-March 2009 since its main source is agriculture with largest emissions occurring in early spring (Fig. 3, see Fig. S7

10   for relative contributions). The highest PNH_4 concentrations were predicted in central Europe. A small contribution (2-10%) from road transport could be seen around the urban areas (Fig. 3, Fig.S7).

3.5 Role of biogenic VOC emissions

Biogenic VOC emissions are known as effective SOA precursors. There are large uncertainties associated with BVOC emission estimates due to the substantial number of compounds and biological

15   sources (Guenther, 2013; Oderbolz et al., 2013). The gas-phase reactions of biogenic species used in the chemical mechanism CB05 in CAMx are given in Table S1. Some of the oxidation reactions produce condensable gases (CG) that might lead to formation of SOA particles (Table S2). The monthly average emissions of isoprene, monoterpenes and sesquiterpenes and their contributions to SOA concentrations in the warm season are shown in Fig. S8. Although isoprene emissions were larger (especially in

20   southern Europe), more SOA was produced by sesquiterpenes and monoterpenes due to their higher SOA yields (Lee et al., 2006; Hallquist et al., 2009; ENVIRON, 2011). SOA was predominantly produced by biogenic precursors and oligomerization processes; the contribution of anthropogenic precursors to SOA was very small.

The model results showed a large increase in SOA (Fig. S9) when BVOC emissions were doubled while

25   PNO_3 and PSO_4 concentrations decreased (Fig. 4). Since the positive correlation between biogenic emissions and SOA is relatively well known, we focused on the role of BVOCs on SIA formation.

Increased BVOC emissions led to greater decreases in PNO_3 (up to 35%, Fig. S10, left panel) than in PSO_4 (<12%, Fig. S10, right panel). The largest decrease in PNO_3 occurred around the Benelux area and northern Italy where concentrations were highest (Fig. 4). PSO_4 decreased mostly in Eastern Europe where SO_2 concentrations were relatively higher. In a study in the eastern U.S, Karambelas (2013) also

5 reported a negative correlation between BVOC emissions and SIA. From the comparison of the base case and no-biogenic emission simulations, the author attributed the increase in SIA concentrations to the increased availability of OH radicals (as a result of elimination of SOA in the absence of BVOC emissions) for oxidation of precursor gases such as NO_2 and SO_2.

We analyzed our results further by investigating the changes in OH radical and production rate of nitric

10 acid (HNO_3) from the two main reaction pathways: $NO_2 + OH$ (daytime) and $N_2O_5 + H_2O$ (nighttime) on the warmest day (14 June 2006) in one grid cell (Payerne, Switzerland) for three different cases: 1) with standard BVOC emissions, 2) with doubled BVOC emissions, 3) with doubled BVOC emissions and without BVOC+NO_3 reactions (see Table S1 for the reactions of BVOCs used in CAMx). OH radical consumption increased when BVOC emissions were doubled, mainly during the daytime (Fig.

15 5a) due to OH oxidation reactions of BVOCs. The decrease in OH radicals most likely caused a reduction in SO_2 oxidation leading to a decrease in PSO_4 concentrations (see Fig. 4, right panel). On the other hand, HNO_3 production from daytime and nighttime reactions as well as PNO_3 concentrations decreased with increasing BVOC emissions (Fig. 5b-5d). Although most of the HNO_3 comes from the daytime reaction of OH with NO_2, since the deposition rate of HNO_3 is very high, the main pathway

20 leading to the formation of PNO_3 is the hydrolysis of N_2O_5 at night, when the temperature is sufficiently low for partitioning to the particle phase. The decrease in HNO_3 production via daytime reaction indicates a decrease in available OH radicals due to BVOC+OH reactions (Table S1 and Fig. 5a). Switching off the reactions with NO_3 radical did not affect the daytime production further, as expected since NO_3 is a nocturnal oxidant (Fig. 5b). On the other hand, HNO_3 production at night decreased with

25 increased BVOC emissions suggesting that the available NO_3 radical decreased due to BVOC + NO_3 reactions (Fig. 5c). The fact that HNO_3 formation at night increased significantly when BVOC + NO_3 reactions were switched off presents further evidence that BVOC+NO_3 reactions were responsible for the changes in PNO_3 concentrations (Fig. 5c-d). Steinbacher et al (2005) showed that isoprene

emissions vanish after sunset and isoprene mixing ratios decline quickly due to chemical reactions with NO_3, O_3 and OH, leaving no isoprene for further reactions during the night. In addition, isoprene oxidation with NO_3 radical produces not only organic nitrates (NTR) but HNO_3 as well (see Table S1). It is therefore more likely that oxidation of terpenes with NO_3 is the main driver for the BVOC effect on

5   PNO_3.

3.6 A case study: The Swiss Plateau

3.6.1 Cold Season (February-March 2009)

The modeled SIA concentrations were relatively high during the first few days in March and during the second half of the period (Fig. 6). Low winds from southwest at the beginning of March (Fig. S3, left

10   panel) led to relatively larger contribution from sources in France as well as from domestic sources to SIA concentrations in the Swiss Plateau. Then, when the wind direction shifted towards the northeast between 16 and 22 March (see Fig. S3), the contribution from Germany became larger.

Domestic sources contribute to PNO_3 concentrations (21%) in the Swiss Plateau as much as sources in Germany (18%) and France (24%) during the whole period of February-March 2009 (Fig. 6, top-middle

15   panel). A large fraction of PNO_3 originates from road transport (40%), while 22% is from shipping emissions in the coastal areas (Fig. 6, top-right panel). Sources from non-industrial combustion (SNAP2) and combustion in energy and transformation industries (SNAP1) contribute 16% and 12%, respectively.

Boundary conditions are predicted to have the largest contribution to PSO_4 in the Swiss Plateau (24%)

20   followed by sources in France (17%), Germany (13%) and the sea areas (13%) (Fig. 6, middle panels). The Swiss sources contribute only to 11%. The main source categories are combustion in energy and transformation industries (SNAP1) and non-industrial combustion (SNAP2) contributing 33% and 23% of total sulfate, respectively.

In the case of PNH_4, domestic sources are clearly the main contributor (73%) followed by the two

25   neighboring countries France (11%) and Germany (10%). These mainly originate from agricultural activities with a small contribution (3%) from road transport (Fig. 6, lower panels).

3.6.2 Warm Season (June 2006)

The magnitude of PNO_3 and PNH_4 concentrations shown in Fig. 7 reflects the temporal evolution of air temperature in June 2006 (Fig. S3, right panel). During the first half of the month, maximum daily temperatures increased from 10^oC to about 30^oC, while both PNO_3 and PNH_4 concentrations decreased.

5 Then both temperatures and nitrate concentrations remained almost the same until the end of June. The wind was blowing from northeast and northwest during the first half of June leading to relatively high contributions to PNO_3 concentrations in the Swiss Plateau from Germany, France and the Benelux countries. Over the whole period, the largest contribution to nitrate was predicted to be from Germany (30%) followed by Switzerland (18%) and France (14%) (Fig. 7). A significant amount was also

10 predicted from marine areas (13%) and the Benelux countries (10%). Our results also suggest that nearly half of PNO_3 originated from road transport (47%), while ship emissions also contributed significantly (about 22%). On the other hand, Switzerland itself was predicted to be the main source for PNH_4 concentrations (71%) with some contribution from Germany (13%) in the first half of June due to northerly winds. Almost all of PNH_4 (96%) originated from agricultural activities.

15 Time series and pie charts for PSO_4 in Fig. 7 indicate a large contribution to sulfate concentrations from remote areas – boundary conditions (34%), marine areas (16%) and the rest of the domain (17%) – especially in the second half of the month, which experienced various wind directions. The contribution of domestic sources to PSO_4 concentrations was very small (3%); the largest contribution among the emission sources was from SNAP1 (45%), followed by SNAP8 (22%).

20 ### 4 Conclusions

In this study, sources of secondary inorganic aerosols in Europe and the role of biogenic emissions on their formation were investigated. Model simulations with CAMx including its PSAT tool were used to estimate the contributions from 10 anthropogenic emission sources as well as from boundary conditions to the concentrations of particulate inorganic nitrate, sulfate and ammonium in Europe during two

25 periods of EMEP measurement campaigns; February-March 2009 (cold season) and June 2006 (warm season).

Road transport (SNAP7) was predicted to be the most important source for PNO_3 with the largest contribution during the cold season over northern Italy. Other important sources were ship emissions (SNAP8), which contributed to particulate inorganic nitrate along the English Channel and Benelux area, and combustion in energy and transformation industries (SNAP1) in Central and Eastern Europe.

5 The model results suggested that PSO_4 in Europe originated from SNAP 1 sources especially in Eastern Europe. The contribution of ship emissions in the Mediterranean and along busy shipping routes was larger during the warm season. A large contribution to sulfate in the eastern part of the domain during the cold season was attributed to inflow from the boundary. Agricultural activities were the dominant source for PNH_4, with a small (2-10%) contribution from road transport.

10 A case study with the Swiss Plateau as receptor, showed how wind speed and direction affected the contribution from various source areas to the particulate nitrate, sulfate and ammonium concentrations in the area. These results suggested that the contribution from the domestic sources to PNO_3 concentrations in the Swiss Plateau was similar to those from Germany and France during the cold season and almost half of it was from road transport. The sources of PSO_4 were mostly of foreign origin

15 from combustion in energy and transformation industries with the domestic contributions of 11% and 3% in winter and summer, respectively. The local agricultural activities were the main source of PNH_4.

An important outcome of this study was the significant role of biogenic VOC emissions on the SIA formation, especially on particulate inorganic nitrate. The sensitivity test carried out during the warm season showed a negative correlation between BVOC emissions and SIA concentrations. Increasing

20 BVOC emissions by a factor of two led to a decrease by 35% and 12% in PNO_3 and PSO_4, respectively. Further investigations using the Chemical Process Analysis tool of CAMx suggested that reactions of terpenes with nitrate radical at night led to a decrease in PNO_3 formation (by reducing HNO_3) when BVOC emissions were doubled. Although OH radical concentration was reduced by oxidation reactions of BVOCs, decreased daytime oxidation of NO_2 with OH did not affect PNO_3 concentrations. On the

25 other hand, reduced availability of OH radical for gas-phase oxidation of SO_2 caused a decrease in PSO_4 concentrations especially over the Aegean and Mediterranean Sea. These results indicated the importance of BVOC emissions not only for secondary organic aerosol formation but also for inorganic aerosols. Considering the challenges in BVOC emission estimates in addition to uncertainties in NH_3

and NO_x emissions, modeled particulate inorganic nitrate concentrations might have larger uncertainties than assumed so far.

Acknowledgements

We acknowledge INERIS for providing various model input data within the EURODELTA III exercise. Anthropogenic emissions were based on TNO and EMEP inventories and data from the GAINS database of IIASA. We thank the European Centre for Medium-Range Weather Forecasts (ECMWF) for the access to the meteorological and the global air quality model data. Calculations of land use data were performed at the Swiss National Supercomputing Centre (CSCS). We appreciate the availability of CAMx model with PSAT and support of RAMBOLL ENVIRON. This work was financially supported by the Swiss Federal Office of Environment (FOEN).

References

Aan de Brugh, J. M. J., Schaap, M., Vignati, E., Dentener, F., Kahnert, M., Sofiev, M., Huijnen, V., and Krol, M. C.: The European aerosol budget in 2006, Atmos. Chem. Phys., 11, 1117-1139, doi:10.5194/acp-11-1117-2011, 2011.

Aas, W., Tsyro, S., Bieber, E., Bergström, R., Ceburnis, D., Ellermann, T., Fagerli, H., Frölich, M., Gehrig, R., Makkonen, U., Nemitz, E., Otjes, R., Perez, N., Perrino, C., Prévôt, A. S. H., Putaud, J. P., Simpson, D., Spindler, G., Vana, M., and Yttri, K. E.: Lessons learnt from the first EMEP intensive measurement periods, Atmos. Chem. Phys., 12, 8073-8094, 10.5194/acp-12-8073-2012, 2012.

Aksoyoglu, S., Keller, J., Barmpadimos, I., Oderbolz, D., Lanz, V. A., Prévôt, A. S. H., and Baltensperger, U.: Aerosol modelling in Europe with a focus on Switzerland during summer and winter episodes, Atmos. Chem. Phys., 11 doi:10.5194/acp-5111-7355-2011, 7355-7373, 2011.

Aksoyoglu, S., Keller, J., Oderbolz, D. C., Barmpadimos, I., Prévôt, A. S. H., and Baltensperger, U.: Sensitivity of ozone and aerosols to precursor emissions in Europe, Int. J. Environ. Pollut., 50 451-459, 10.1504/ijep.2012.051215, 2012.

Aksoyoglu, S., Baltensperger, U., and Prévôt, A. S. H.: Contribution of ship emissions to the concentration and deposition of air pollutants in Europe, Atmos. Chem. Phys., 16, 1895-1906, 10.5194/acp-16-1895-2016, 2016.

Ayres, B. R., Allen, H. M., Draper, D. C., Brown, S. S., Wild, R. J., Jimenez, J. L., Day, D. A., Campuzano-Jost, P., Hu, W., de Gouw, J., Koss, A., Cohen, R. C., Duffey, K. C., Romer, P., Baumann, K., Edgerton, E., Takahama, S., Thornton, J. A., Lee, B. H., Lopez-Hilfiker, F. D., Mohr, C., Wennberg, P. O., Nguyen, T. B., Teng, A., Goldstein, A. H., Olson, K., and Fry, J. L.: Organic nitrate aerosol formation via NO_3 + biogenic volatile organic compounds in the southeastern United States, Atmos. Chem. Phys., 15, 13377-13392, 10.5194/acp-15-13377-2015, 2015.

Barmpadimos, I., Keller, J., Oderbolz, D., Hueglin, C., and Prévôt, A. S. H.: One decade of parallel fine ($PM_{2.5}$) and coarse (PM_{10}–$PM_{2.5}$) particulate matter measurements in Europe: trends and variability, Atmos. Chem. Phys., 12, 3189-3203, 10.5194/acp-12-3189-2012, 2012.

Benedetti, A., Morcrette, J. J., Boucher, O., Dethof, A., Engelen, R. J., Fisher, M., Flentje, H., Huneeus, N., Jones, L., Kaiser, J. W., Kinne, S., Mangold, A., Razinger, M., Simmons, A. J., and Suttie, M.: Aerosol analysis and forecast in the European Centre for Medium-Range Weather Forecasts Integrated Forecast System: 2. Data assimilation, J. Geophys. Res., 114, D1325 10.1029/2008JD011115, 2009.

Bessagnet, B., Colette, A., Meleux, F., Rouïl, L., Ung, A., Favez, O., Cuvelier, C., Thunis, P., Tsyro, S., Stern, R., Manders, A., Kranenburg, R., Aulinger, A., Bieser, J., Mircea, M., Briganti, G., Cappelletti, A., Calori, G., Finardi, S., Silibello, C., Ciarelli, G., Aksoyoglu, S., Prévôt, A. S. H., Pay, M. T., Baldasano, J. M., García Vivanco, M., Garrido, J. L., Palomino, I., Martin, F., Pirovano, G., Roberts, P., Gonzalez, L., White, L., Menut, L., Dupont, J. C., Carnevale, C., and Pederzoli, A.: The EURODELTA III exercise – Model evaluation with observations issued from the 2009 EMEP intensive period and standard measurements in Feb/Mar 2009, EMEP, Oslo, Norway Technical Report MSC-W 1/2014, 2014.

Boyd, C. M., Sanchez, J., Xu, L., Eugene, A. J., Nah, T., Tuet, W. Y., Guzman, M. I., and Ng, N. L.: Secondary organic aerosol formation from the β-pinene+NO_3 system: effect of humidity and peroxy radical fate, Atmos. Chem. Phys., 15, 7497-7522, 10.5194/acp-15-7497-2015, 2015.

Carlton, A. G., Wiedinmyer, C., and Kroll, J. H.: A review of Secondary Organic Aerosol (SOA) formation from isoprene, Atmos. Chem. Phys., 9, 4987-5005, 2009.

Chang, J. S., Brost, R. A., Isaksen, I. S. A., Madronich, S., Middleton, P., Stockwell, W. R., and Walcek, C. J.: A three-dimensional eulerian acid deposition model : Physical concepts and formulation,
5   J. Geophys. Res., 92, 14681-14700, 10.1029/JD092iD12p14681,1987.

Ciarelli, G., Aksoyoglu, S., Crippa, M., Jimenez, J. L., Nemitz, E., Sellegri, K., Äijälä, M., Carbone, S., Mohr, C., O'Dowd, C., Poulain, L., Baltensperger, U., and Prévôt, A. S. H.: Evaluation of European air quality modelled by CAMx including the volatility basis set scheme, Atmos. Chem. Phys., 16, 10313-10332, 10.5194/acp-16-10313-2016, 2016.

10   Crippa, M., Canonaco, F., Lanz, V. A., Äijälä, M., Allan, J. D., Carbone, S., Capes, G., Ceburnis, D., Dall'Osto, M., Day, D. A., DeCarlo, P. F., Ehn, M., Eriksson, A., Freney, E., Hildebrandt Ruiz, L., Hillamo, R., Jimenez, J. L., Junninen, H., Kiendler-Scharr, A., Kortelainen, A. M., Kulmala, M., Laaksonen, A., Mensah, A. A., Mohr, C., Nemitz, E., O'Dowd, C., Ovadnevaite, J., Pandis, S. N., Petäjä, T., Poulain, L., Saarikoski, S., Sellegri, K., Swietlicki, E., Tiitta, P., Worsnop, D. R.,
15   Baltensperger, U., and Prévôt, A. S. H.: Organic aerosol components derived from 25 AMS data sets across Europe using a consistent ME-2 based source apportionment approach, Atmos. Chem. Phys., 14, 6159-6176, 10.5194/acp-14-6159-2014, 2014.

Denier van der Gon, H. A. C., Bergström, R., Fountoukis, C., Johansson, C., Pandis, S. N., Simpson, D., and Visschedijk, A. J. H.: Particulate emissions from residential wood combustion in Europe – revised
20   estimates and an evaluation, Atmos. Chem. Phys., 15, 6503-6519, 10.5194/acp-15-6503-2015, 2015.

EEA: Air Quality in Europe, 2014 Report, doi:10.2800/22847, 2014

Emmerson, K. M., Galbally, I. E., Guenther, A. B., Paton-Walsh, C., Guerette, E. A., Cope, M. E., Keywood, M. D., Lawson, S. J., Molloy, S. B., Dunne, E., Thatcher, M., Karl, T., and Maleknia, S. D.: Current estimates of biogenic emissions from eucalypts uncertain for southeast Australia, Atmos. Chem.
25   Phys., 16, 6997-7011, 10.5194/acp-16-6997-2016, 2016.

ENVIRON: User's Guide, Comprehensive Air Quality Model with Extensions (CAMx), Version 5.40, Environ International Corporation, California., 2011.

Fry, J. L., Kiendler-Scharr, A., Rollins, A. W., Brauers, T., Brown, S. S., Dorn, H. P., Dubé, W. P., Fuchs, H., Mensah, A., Rohrer, F., Tillmann, R., Wahner, A., Wooldridge, P. J., and Cohen, R. C.: SOA from limonene: role of NO_3 in its generation and degradation, Atmos. Chem. Phys., 11, 3879-3894, 10.5194/acp-11-3879-2011, 2011.

5   Fuzzi, S., Baltensperger, U., Carslaw, K., Decesari, S., Denier van der Gon, H., Facchini, M. C., Fowler, D., Koren, I., Langford, B., Lohmann, U., Nemitz, E., Pandis, S., Riipinen, I., Rudich, Y., Schaap, M., Slowik, J. G., Spracklen, D. V., Vignati, E., Wild, M., Williams, M., and Gilardoni, S.: Particulate matter, air quality and climate: lessons learned and future needs, Atmos. Chem. Phys., 15, 8217-8299, 10.5194/acp-15-8217-2015, 2015.

10 Guenther, A. B., Jiang, X., Heald, C. L., Sakulyanontvittaya, T., Duhl, T., Emmons, L. K., and Wang, X.: The Model of Emissions of Gases and Aerosols from Nature version 2.1 (MEGAN2.1): an extended and updated framework for modeling biogenic emissions, Geosci. Model Dev., 5, 1471-1492, 10.5194/gmd-5-1471-2012, 2012.

Guenther, A.: Biological and Chemical Diversity of Biogenic Volatile Organic Emissions into the
15 Atmosphere, ISRN Atmos. Sci., 2013, 27, 10.1155/2013/786290, 2013.

Guevara, M., Pay, M. T., Martínez, F., Soret, A., Denier van der Gon, H., and Baldasano, J. M.: Inter-comparison between HERMESv2.0 and TNO-MACC-II emission data using the CALIOPE air quality system (Spain), Atmos. Environ., 98, 134-145, http://dx.doi.org/10.1016/j.atmosenv.2014.08.067, 2014.

Hallquist, M., Wenger, J. C., Baltensperger, U., Rudich, Y., Simpson, D., Claeys, M., Dommen, J.,
20 Donahue, N. M., George, C., Goldstein, A. H., Hamilton, J. F., Herrmann, H., Hoffmann, T., Iinuma, Y., Jang, M., Jenkin, M. E., Jimenez, J. L., Kiendler-Scharr, A., Maenhaut, W., McFiggans, G., Mentel, T. F., Monod, A., Prévôt, A. S. H., Seinfeld, J. H., Surratt, J. D., Szmigielski, R., and Wildt, J.: The formation, properties and impact of secondary organic aerosol: current and emerging issues, Atmos. Chem. Phys., 9 5155-5235, 2009.

25 Inness, A., Baier, F., Benedetti, A., Bouarar, I., Chabrillat, S., Clark, H., Clerbaux, C., Coheur, P., Engelen, R. J., Errera, Q., Flemming, J., George, M., Granier, C., Hadji-Lazaro, J., Huijnen, V., Hurtmans, D., Jones, L., Kaiser, J. W., Kapsomenakis, J., Lefever, K., Leitão, J., Razinger, M., Richter, A., Schultz, M. G., Simmons, A. J., Suttie, M., Stein, O., Thépaut, J. N., Thouret, V., Vrekoussis, M.,

Zerefos, C., and the MACC team: The MACC reanalysis: an 8 yr data set of atmospheric composition, Atmos. Chem. Phys., 13, 4073-4109, 10.5194/acp-13-4073-2013, 2013.

Kanakidou, M., Seinfeld, J. H., Pandis, S. N., Barnes, I., Dentener, F. J., Facchini, M. C., Van Dingenen, R., Ervens, B., Nenes, A., Nielsen, C. J., Swietlicki, E., Putaud, J. P., Balkanski, Y., Fuzzi, S., Horth, J., Moortgat, G. K., Winterhalter, R., Myhre, C. E. L., Tsigaridis, K., Vignati, E., Stephanou, E. G., and Wilson, J.: Organic aerosol and global climate modelling: a review, Atmos. Chem. Phys., 5, 1053-1123, 2005.

Karambelas, A.: The Interactions of Biogenic and Anthropogenic Gaseous Emissions with Respect to Aerosol Formation in the United States, Master of Science, Department of Atmospheric and Oceanic Sciences, University of Wisconsin, Madison, 2013.

Kuenen, J., Denier van der Gon, H., Visschedijk, A., van der Brugh, H., and van Gijlswijk, R.: MACC European emission inventory for the years 2003-2007, The Netherlands, TNO-060-UT-2011-00588, 2011.

Lee, A., Goldstein, A. H., Kroll, J. H., Ng, N. L., Varutbangkul, V., Flagan, R. C., and Seinfeld, J. H.: Gas-phase products and secondary aerosol yields from the photooxidation of 16 different terpenes, J. Geophys. Res., 111, D17305, 10.1029/2006JD007050, 2006.

Nenes, A., Pandis, S. N., and Pilinis, C.: ISORROPIA: A new thermodynamic equilibrium model for multiphase multicomponent inorganic aerosols, Aquat. Geochem., 4, 123-152, 1998.

Oderbolz, D. C., Aksoyoglu, S., Keller, J., Barmpadimos, I., Steinbrecher, R., Skjøth, C. A., Plaß-Dülmer, C., and Prévôt, A. S. H.: A comprehensive emission inventory of biogenic volatile organic compounds in Europe: improved seasonality and land-cover, Atmos. Chem. Phys., 13 1689-1712, 10.5194/acp-13-1689-2013, 2013.

Revuelta, M. A., Harrison, R. M., Núñez, L., Gomez-Moreno, F. J., Pujadas, M., and Artíñano, B.: Comparison of temporal features of sulphate and nitrate at urban and rural sites in Spain and the UK, Atmos. Environ., 60, 383-391, http://dx.doi.org/10.1016/j.atmosenv.2012.07.004, 2012.

Sartelet, K. N., Couvidat, F., Seigneur, C., and Roustan, Y.: Impact of biogenic emissions on air quality over Europe and North America, Atmos. Environ., 53, 131-141, http://dx.doi.org/10.1016/j.atmosenv.2011.10.046, 2012.

Schaap, M., van Loon, M., ten Brink, H. M., Dentener, F. J., and Builtjes, P. J. H.: Secondary inorganic aerosol simulations for Europe with special attention to nitrate, Atmos. Chem. Phys., 4, 857-874, 10.5194/acp-4-857-2004, 2004.

Sciare, J., d'Argouges, O., Zhang, Q. J., Sarda-Estève, R., Gaimoz, C., Gros, V., Beekmann, M., and Sanchez, O.: Comparison between simulated and observed chemical composition of fine aerosols in Paris (France) during springtime: contribution of regional versus continental emissions, Atmos. Chem. Phys., 10, 11987-12004, 10.5194/acp-10-11987-2010, 2010.

Sindelarova, K., Granier, C., Bouarar, I., Guenther, A., Tilmes, S., Stavrakou, T., Müller, J. F., Kuhn, U., Stefani, P., and Knorr, W.: Global data set of biogenic VOC emissions calculated by the MEGAN model over the last 30 years, Atmos. Chem. Phys., 14, 9317-9341, 10.5194/acp-14-9317-2014, 2014.

Squizzato, S., Masiol, M., Brunelli, A., Pistollato, S., Tarabotti, E., Rampazzo, G., and Pavoni, B.: Factors determining the formation of secondary inorganic aerosol: a case study in the Po Valley (Italy), Atmos. Chem. Phys., 13, 1927-1939, 10.5194/acp-13-1927-2013, 2013.

Steinbacher, M., Dommen, J., Ordonez, C., Reimann, S., Grueebler, F. C., Staehelin, J., Andreani-Aksoyoglu, S., and Prévôt, A. S. H.: Volatile Organic Compounds in the Po Basin. Part B: Biogenic VOCs, J. Atmos. Chem., 51, 293-315, DOI: 10.1007/s10874-005-3577-0, 2005.

Strader, R., Lurmann, F., and Pandis, S. N.: Evaluation of secondary organic aerosol formation in winter, Atmos. Environ., 33, 4849-4863, 1999.

Vaughan, A. R., Lee, J. D., Misztal, P. K., Metzger, S., Shaw, M. D., Lewis, A. C., Purvis, R. M., Carslaw, D. C., Goldstein, A. H., Hewitt, C. N., Davison, B., Beevers, S. D., and Karl, T. G.: Spatially resolved flux measurements of NOx from London suggest significantly higher emissions than predicted by inventories, Faraday Discussions, 189, 455-472, 10.1039/C5FD00170F, 2016.

Vestreng, V., Myhre, G., Fagerli, H., Reis, S., and Tarrasón, L.: Twenty-five years of continuous sulphur dioxide emission reduction in Europe, Atmos. Chem. Phys., 7, 3663-3681, 10.5194/acp-7-3663-2007, 2007.

Viana, M., Kuhlbusch, T. A. J., Querol, X., Alastuey, A., Harrison, R. M., Hopke, P. K., Winiwarter, W., Vallius, M., Szidat, S., Prévôt, A. S. H., Hueglin, C., Bloemen, H., Wåhlin, P., Vecchi, R., Miranda,

A. I., Kasper-Giebl, A., Maenhaut, W., and Hitzenberger, R.: Source apportionment of particulate matter in Europe: A review of methods and results, J. Aerosol Sci., 39, 827-849, 2008.

Wang, Y., Zhang, Q. Q., He, K., Zhang, Q., and Chai, L.: Sulfate-nitrate-ammonium aerosols over China: response to 2000–2015 emission changes of sulfur dioxide, nitrogen oxides, and ammonia, Atmos. Chem. Phys., 13, 2635-2652, 10.5194/acp-13-2635-2013, 2013.

Xu, L., Guo, H., Boyd, C. M., Klein, M., Bougiatioti, A., Cerully, K. M., Hite, J. R., Isaacman-VanWertz, G., Kreisberg, N. M., Knote, C., Olson, K., Koss, A., Goldstein, A. H., Hering, S. V., de Gouw, J., Baumann, K., Lee, S.-H., Nenes, A., Weber, R. J., and Ng, N. L.: Effects of anthropogenic emissions on aerosol formation from isoprene and monoterpenes in the southeastern United States, Proceedings of the National Academy of Sciences, 112, 37-42, 10.1073/pnas.1417609112, 2015.

Yarwood, G., Rao, S., Yocke, M., and Whitten, G. Z.: Updates to the Carbon Bond chemical mechanism: CB05 Yocke & Company, Novato, CA 94945RT-04-00675, 2005.

Zhang, L., Brook, J. R., and Vet, R.: A revised parameterization for gaseous dry deposition in air-quality models, Atmos. Chem. Phys., 3 2067-2082, 10.5194/acp-3-2067-2003, 2003.

Table 1: Source categories used in this study

Source categories	
SNAP1	Combustion in energy and transformation industries
SNAP2	Non-industrial combustion
SNAP3	Combustion in manufacturing industry
SNAP4	Production processes
SNAP5	Extraction and distribution of fossil fuels and geothermal energy
SNAP6	Solvent and other product use
SNAP7	Road transport
SNAP8	Other mobile sources and machinery
SNAP9	Waste treatment and disposal
SNAP10	Agriculture
Boundary conditions (concentrations on the lateral model boundaries)	
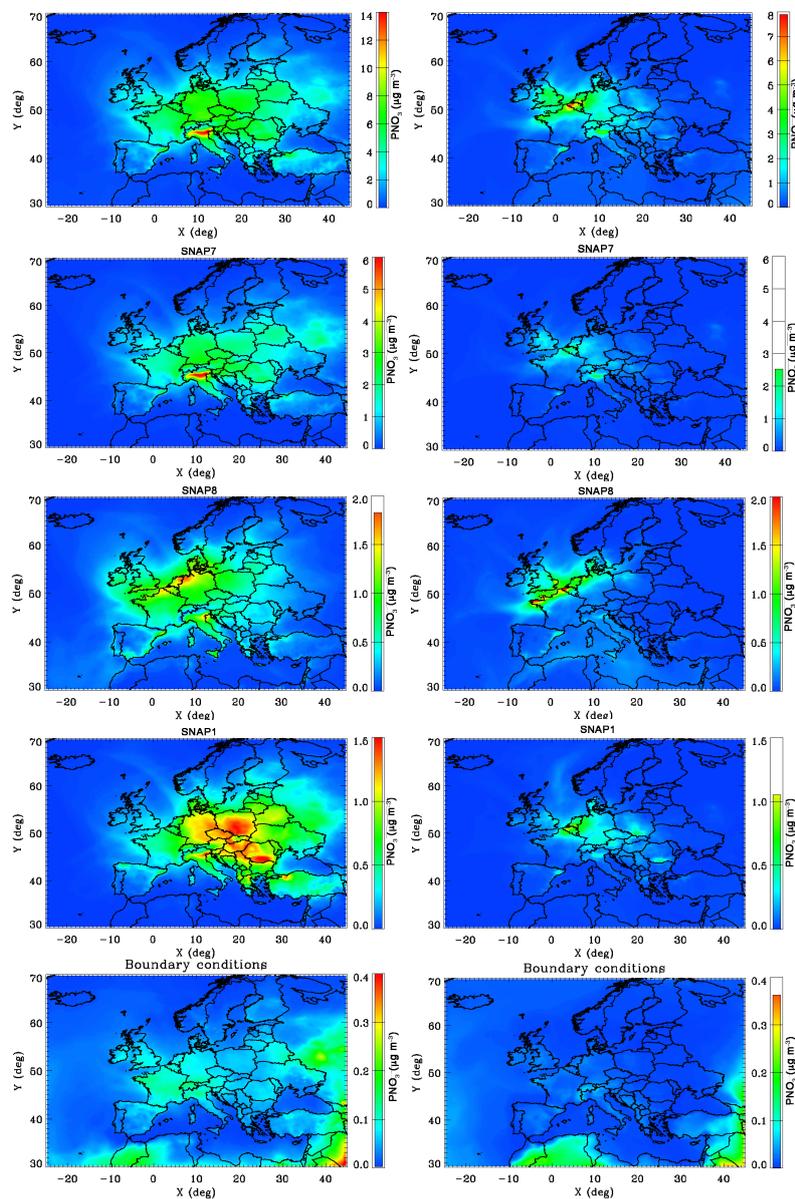
Figure 1: Average concentrations of PNO$_3$ and contributions from road transport (SNAP7), ships (SNAP8), combustion in energy and transformation industries (SNAP1) and boundary conditions in February-March 2009 (left) and in June 2006 (right).
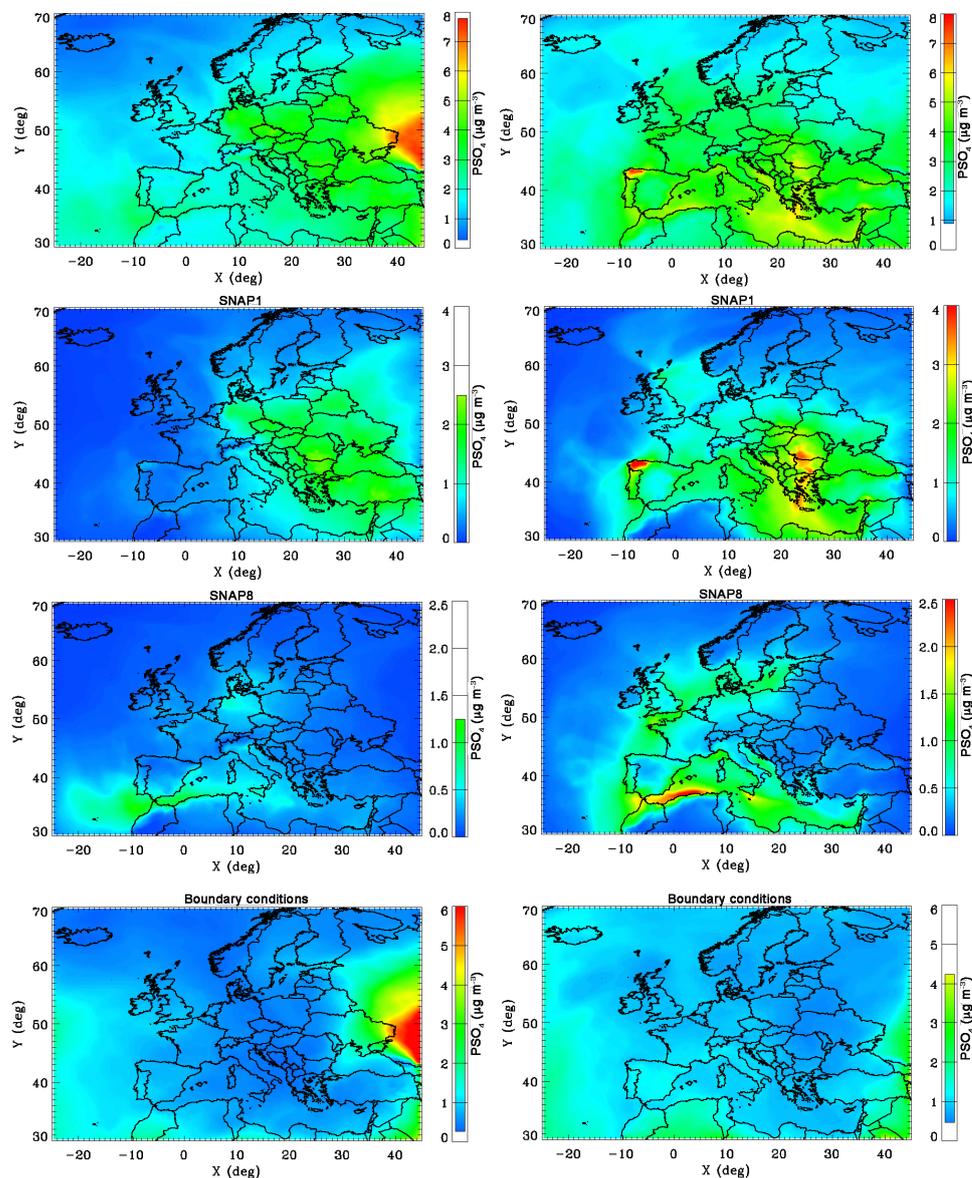
Figure 2: Average concentrations of PSO₄ and contributions from combustion in energy and transformation industries (SNAP1), ships (SNAP8) and boundary conditions in February-March 2009 (left) and in June 2006 (right).
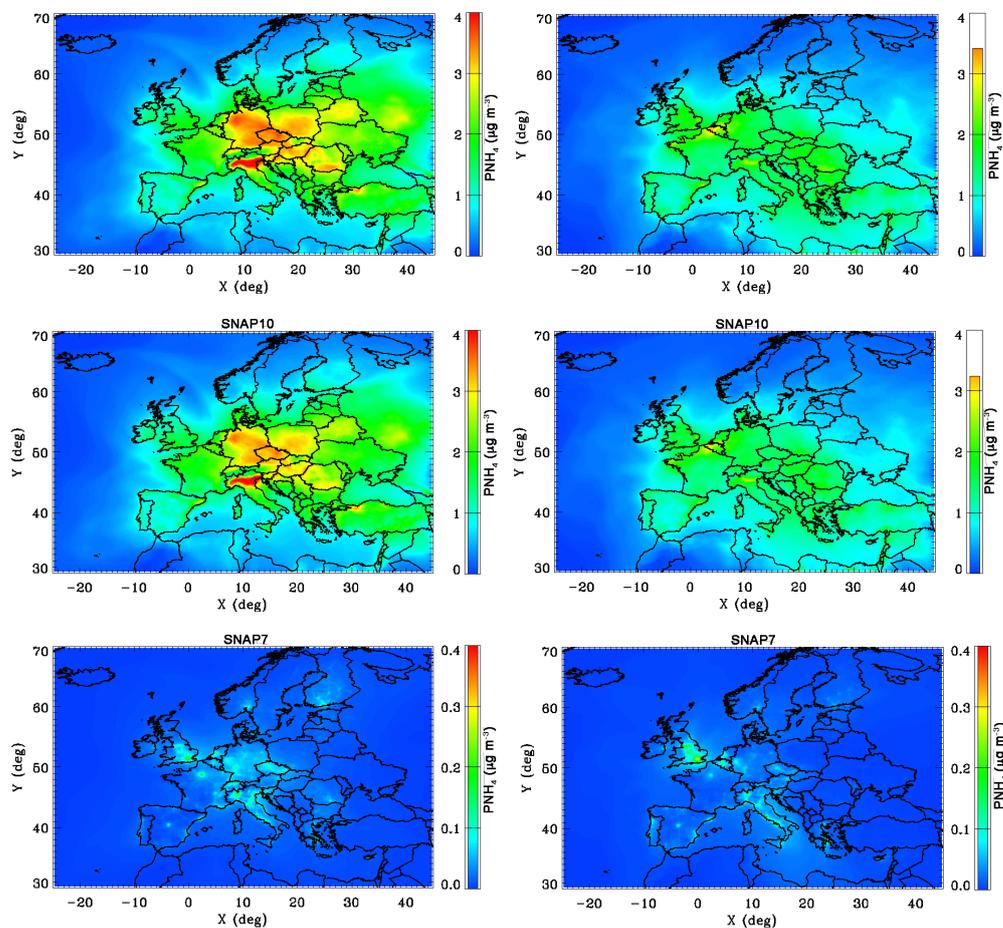
Figure 3: Average concentrations of PNH$_4$ and contributions from agriculture (SNAP10) and road transport (SNAP7) in February-March 2009 (left) and in June 2006 (right).
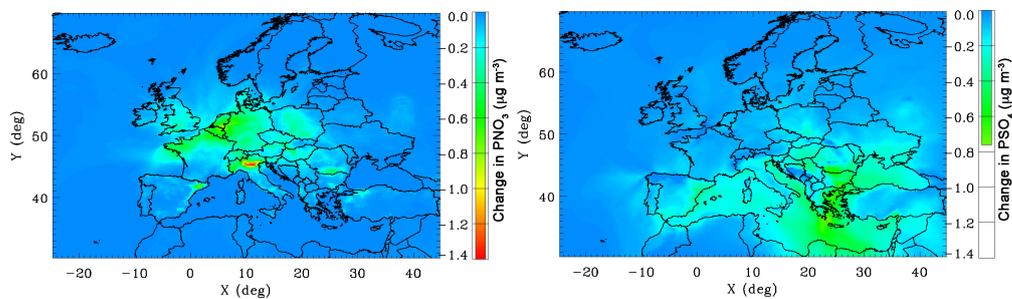
Figure 4: Change in PNO₃ (left) and PSO₄ (right) concentrations in June 2006 when BVOC emissions were doubled.
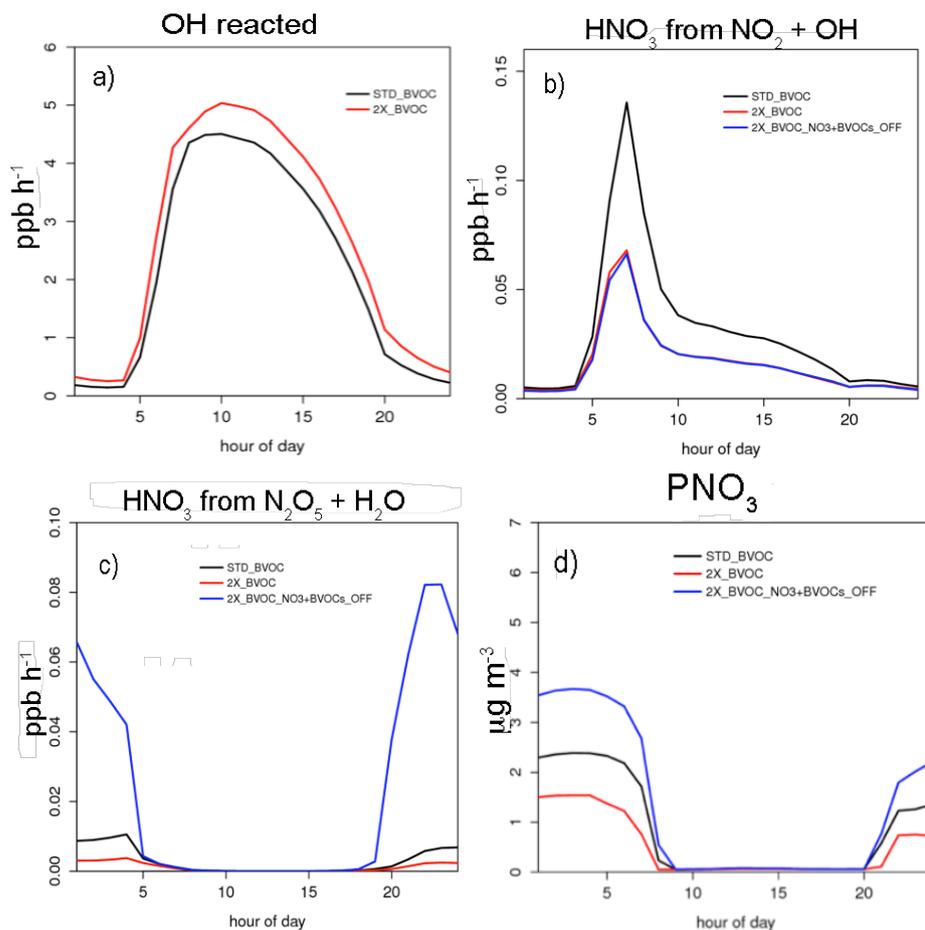
Figure 5: Changes in diurnal variation of a) reaction rate of OH, b) production rate of HNO$_3$ from daytime reaction, c) production rate of HNO$_3$ from nighttime reaction, d) PNO$_3$ concentration. Black: with standard BVOC, red: with doubled BVOC, blue: when BVOC emissions were doubled and BVOC+NO$_3$ reactions were switched off (Payerne, 14 June 2006).
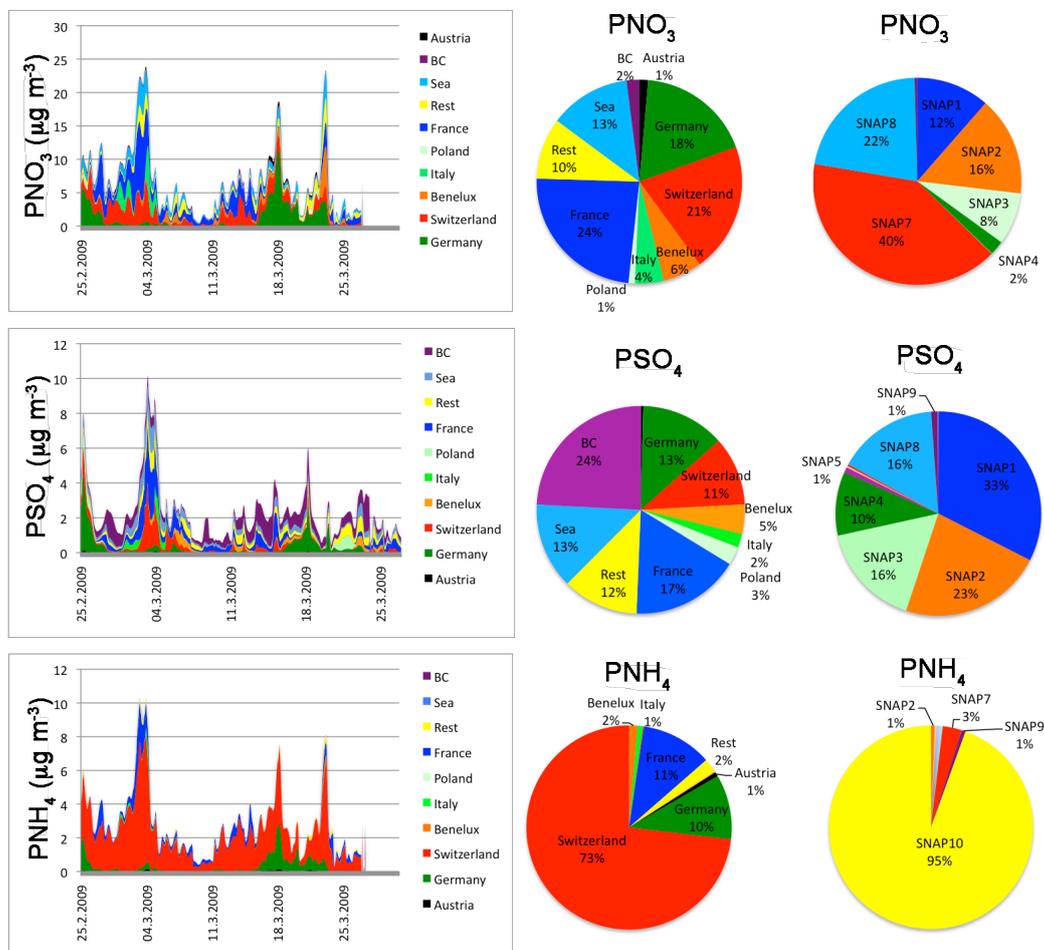
Figure 6: Contributions from various source regions (time series on the left, pie-charts in the middle) and categories (pie-charts on the right) to the concentrations of PNO₃ (top), PSO₄ (middle) and PNH₄ (bottom) in the Swiss Plateau during February-March 2009.
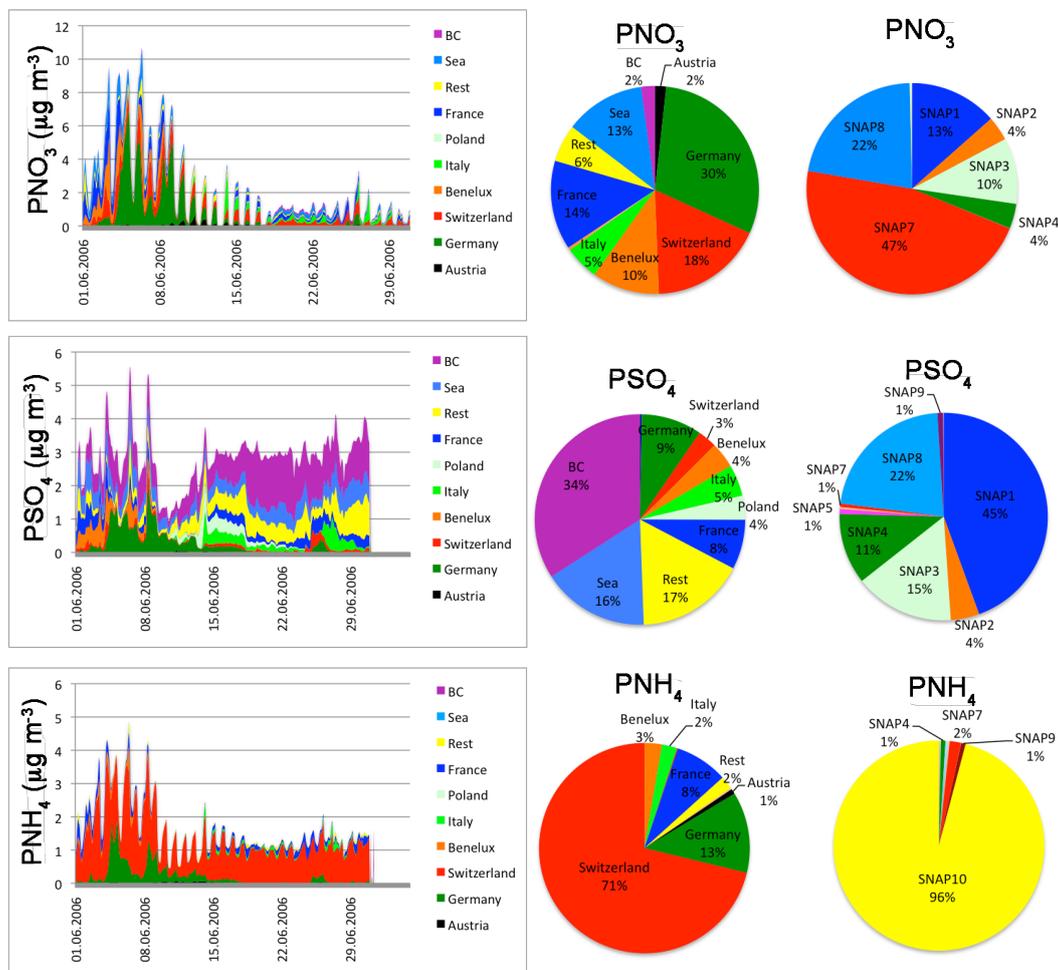
Figure 7: Contributions from various source regions (time series on the left, pie-charts in the middle) and categories (pie-charts on the right) to concentrations of PNO_3 (top), PSO_4 (middle) and PNH_4 (bottom) in the Swiss Plateau during June 2006.